Overcoming the LIT

Niels R. Walet*
Department of Physics and Astronomy, University of Manchester, Manchester M13 9PL, UK
(Dated: May 25, 2021)

Tackling the LIT through a model

I. INTRODUCTION

II. THE CALCULATION OF THE CROSS SECTION

[[[Stuff missing]]]

The key aspect of the calculation are the dynamical polarisabilities [1, 2], which for a single channel read

$$F(\omega,\boldsymbol{q}) = \int \mathrm{d}\boldsymbol{k}\, \langle\psi_0|O^\dagger(\boldsymbol{q})|\psi_{\boldsymbol{k}}\rangle\langle\psi_{\boldsymbol{k}}|O(\boldsymbol{q})|\psi_0\rangle\delta(E_f-E_0-\omega)\,. \tag{1}$$

Here the important aspect is the normalisation of the integrand and wave functions:

$$\int \mathrm{d}\boldsymbol{k}\, |\psi_{\boldsymbol{k}}\rangle\, \langle\psi_{\boldsymbol{k}}| = \widehat{1}\,. \tag{2}$$

The LIT transform of the polarisabilities is defined as

$$L(\sigma) = \int \mathrm{d}\omega \frac{F(\omega,\boldsymbol{q})}{(\omega-\sigma_R)^2+\sigma_I^2} \tag{3}$$

where we take $\sigma_I > 0$, but will not restrict σ_R. Using completeness, this can be written as

$$(H-E_0-\sigma)\left|\tilde{\psi}\right\rangle = O(\boldsymbol{q})\,|\psi_0\rangle\,, \tag{4}$$

$$L = \left\langle\tilde{\psi}\middle|\tilde{\psi}\right\rangle\,. \tag{5}$$

.

If we are using a finite basis of square-integrable functions, we can write the LIT decomposition in terms of the eigenfunctions ϕ_i and eigenvalues E_i of the matrix representation of the Hamiltonian, an approach discussed in [2], i.e.,

$$L(\sigma) = \sum_i \frac{|\gamma_i|^2}{(E_i-E_0-\sigma_R)^2+\sigma_I^2}\,. \tag{6}$$

It is suggested there that increasing the number of basis functions leads to a denser spectrum, and thus a better LIT transformation; this is actually a subtle issue, as shown below. In the standard works on the LIT, one usually works with a finite σ_I, and tries to invert the LIT by ignoring small fluctuations, helped by the finite σ_I. This is like squinting at the function, and we expect that there is a price to pay in the inversion. The reason this price can be small is the smoothness of the polarisabilities. Nevertheless, we find it harder to control the smoothness of our numerical results, especially when using Gaussian basis sets. In that case, we would really like to take a stab at the limit $\sigma_I \to 0$, and one practical approach to approximate this limit is discussed here. To this end we shall mainly investigate the integrated strength function $T(\omega) = \int \mathrm{d}\omega' F(\boldsymbol{q},\omega')$, rather than F. In the next section we illustrate this approach with a simple one dimensional potential.

III. A SIMPLE MODEL

We shall use the one-dimensional Pöschl-Teller potential [3] as a test example (this potential is discussed in some detail in the textbook Ref. [4]). We consider the Hamiltonian

$$H = -\frac{1}{2}\frac{\mathrm{d}^2}{\mathrm{d}x^2} - \frac{\lambda(\lambda+1)}{2\cosh^2 x}\,. \tag{7}$$

The ground state is in general $\psi_0(x) = (\cosh x)^(-\lambda)$ with eigenvalue $-\lambda^2/2$, and a first excited state $\psi_1(x) = \sinh(x)\psi_0(x)$ appears at energy $-(\lambda-1)^2/2$ for $\lambda > 1$.

We consider the single bound state case for $\lambda = 1$, which has a bound state at energy $-1/2$ with normalised eigenfunction

$$\psi_0(x) = \frac{1}{\sqrt{2}}\frac{1}{\cosh x}\,.$$

We shall look at the "photo-excitation" cross section for this model potential in the dipole approximation, $O(q) = \lambda q x$, and we shall ignore below any "trivial" multiplicative term $(\lambda q)^2$.

The operator x creates a state in the positive energy continuum, this means that we will need to know the odd-parity positive energy spectrum for energy $E = k^2/2$, [5]

$$\psi_k^{\mathrm{o}} = \frac{1}{\sqrt{1+k^2}}\left(k\sin(kx) + \tanh(x)\cos(kx)\right)\,. \tag{8}$$

We clearly see that these wave functions approach $\sin(kx \pm \delta_k/2)$ for $x \to \pm\infty$, with the phase shift $\delta_k = 2\arctan 1/k$.

* Niels.Walet@manchester.ac.uk

A. Momentum-space basis

We can calculate the generalised Fourier-decomposition of $x\psi_0$ in closed form,

$$\psi_1(k) = \int_{-\infty}^{\infty} \psi_k^{\rm o}(x) x \psi_0(x)\, {\rm d}x = \frac{\pi\, {\rm sech}\,(\pi k/2)}{\sqrt{2}\sqrt{k^2+1}}\,. \qquad (9)$$

It is quite illustrative to calculate the inverse Fourier transform in detail,

$$I = \frac{1}{2\pi}\int_{-\infty}^{\infty} \psi_k^{\rm o}(x) \frac{\pi\, {\rm sech}\,(\pi k/2)}{\sqrt{2}\sqrt{k^2+1}}\, {\rm d}k\,. \qquad (10)$$

This integral is tackled by contour integration. Closing the contour in the lower half plane, we have poles at $k = -(2n+1)i$, $n \in \mathbb{N}$. Taking the residues, we find

$$\begin{aligned} I =& \frac{1}{\sqrt{2}}\Bigg(\sinh(x) + x\,{\rm sech}(x) + \\ & \frac{1}{2}\sum_{n=1}^{\infty}(-1)^n(2n+1)\frac{(n-1)!}{(n+1)!}\sinh((2n+1)x) - \\ & \frac{1}{2}\tanh(x)\sum_{n=1}^{\infty}(-1)^n\frac{(n-1)!}{(n+1)!}\cosh((2n+1)x)\Bigg) \\ =& \frac{1}{\sqrt{2}} x\,{\rm sech}\, x = \psi_0(x)\,. \end{aligned} \qquad (11)$$

B. check on normalisation

So we have now validated the Fourier and the inverse transformation. The only thing to check is normalisation. We know that

$$\int_{-\infty}^{\infty} x^2\, {\rm sech}^2\, x\, {\rm d}x = \pi^2/6\,. \qquad (12)$$

Comparing that to the most obvious definition of the same integral in k-space,

$$\frac{1}{2\pi}\int_{-\infty}^{\infty} \frac{\pi^2\, {\rm sech}^2\,(k\pi/2)}{(k^2+1)}{\rm d}k = \frac{\pi^2}{6}\,, \qquad (13)$$

we see that this is indeed a consistent normalisation.

C. strength function

The bench mark for all the calculations performed here is the known strength function, which from Eq. (1) becomes

$$F(\omega) = \frac{\pi^2}{2}\frac{1}{\sqrt{2\omega}}\frac{{\rm sech}\left(\pi\sqrt{\omega/2}\right)^2}{1+2\omega}\,, \qquad (14)$$

where $\omega = k^2/2$, and the integrated strength

$$T(\omega) = \int_0^{\omega} F(\omega'){\rm d}\omega' = \int_0^{\sqrt{2\omega}} |\psi_1(k)|^2\, {\rm d}k\,, \qquad (15)$$

see Fig. 1 for a representation. The most important message from that graph is the saturation of the strength function, which can be easily be proven to equal the norm squared of $x\,|\psi_0\rangle$, $\pi^2/12 \approx 0.822467$.

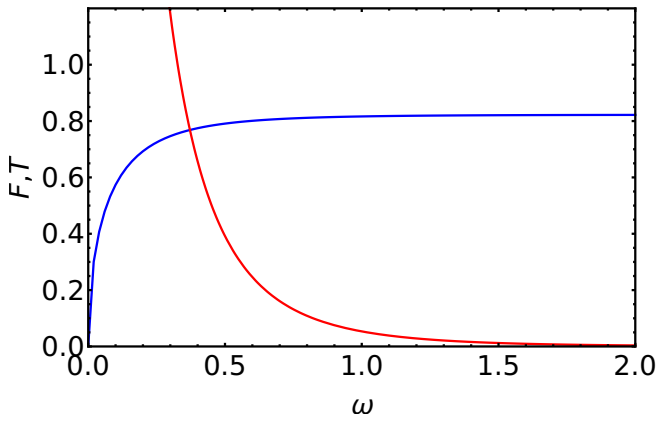

FIG. 1. The baseline for F (red curve) and the integrated strength T (blue curve)

We can now do the same for the LIT transform of the strength function expressed as a k space integral,

$$\begin{aligned} L(\sigma) &= \langle\psi_0|xG_{\rm reg}(\sigma)^\dagger G_{\rm reg}(\sigma)x|\psi_0\rangle \\ &= \frac{1}{2\pi}\frac{\pi^2}{2}\left[\int_{-\infty}^{\infty}\frac{{\rm sech}^2\,(k\pi/2)}{(k^2+1)\left((k^2/2-\sigma_R)^2+\sigma_I^2\right)}{\rm d}k\right]_{\rm reg}\,, \end{aligned} \qquad (16)$$

where $\sigma = \sigma_R + i\sigma_I$. The subscript "reg" denotes that we only keep the part that remains finite as $\sigma_I \to 0$, or the L^2 part of the inversion, see below.

We write separately the contribution due to the Green's function poles, and the remaining residues at the poles of the wave function, $k = -(2n+1)i$. The latter gives the sum

$$
\begin{aligned}
S_1(\sigma) =& \frac{\pi^2}{3\left(4\sigma_I^2+(2\sigma_R+1)^2\right)} + \frac{16|\sigma|^4+32\sigma_R|\sigma|^2-56|\sigma|^2+272\sigma_R^2+200\sigma_R+49}{\left(4\sigma_I^2+(2\sigma_R+1)^2\right)^3} - \\
& \sum_{i=1}^{\infty} \frac{(2i+1)\left(\left(2\sigma_R+(2i+1)^2\right)(2\sigma_R+12i(i+1)+1)+4\sigma_I^2\right)}{i^2(i+1)^2\left(\left((2i+1)^2+2\sigma_R\right)^2+4\sigma_I^2\right)^2} \\
=& \frac{1/4+\pi^2/6}{(1/2+\sigma)(1/2+\sigma^*)} + \frac{6}{((1/2+\sigma)(1/2+\sigma^*))^2} + \frac{8\sigma_I^2}{((1/2+\sigma)(1/2+\sigma^*))^3} \\
& + \frac{1}{4\sqrt{2}\sigma_I}\,\mathrm{Re}\left(\frac{\psi^{(1)}\left(\frac{1}{2}-\frac{i\sqrt{\sigma}}{\sqrt{2}}\right)-\psi^{(1)}\left(\frac{1}{2}+\frac{i\sqrt{\sigma}}{\sqrt{2}}\right)}{\sqrt{\sigma}(1/2+\sigma)}\right), \qquad (17)
\end{aligned}
$$

where $\psi^{(n)}$ is the polygamma function. The factors $(1/2+\sigma)$ can be interpreted as the effect of the bound-state pole at $E=-1/2$.

This expression has a well-behaved limit for $\sigma_I \to 0$,

$$
\begin{aligned}
S_1(\sigma_R) =& \frac{\pi^2}{3(2\sigma_R+1)^2} \\
& + \frac{(6\sigma_R+1)\,\mathrm{Im}(\psi^{(1)}(1/2+i\sqrt{\sigma_R/2}))}{2\sqrt{2}\sigma_R^{3/2}(2\sigma_R+1)^2} \\
& + \frac{\mathrm{Re}(\psi^{(2)}(1/2+i\sqrt{\sigma_R/2}))}{4\sigma_R\,(2\sigma_R+1)}.
\end{aligned}
$$

The poles of the GF give a contribution to the integral in (10) of

$$
S_2(\sigma) = -\frac{1}{2\sqrt{2}\sigma_I}\left(\frac{\mathrm{sech}^2\left(\pi\sqrt{\sigma/2}\right)}{\sqrt{\sigma}(2\sigma+1)} + \frac{\mathrm{sech}^2\left(\pi\sqrt{\sigma^*/2}\right)}{\sqrt{\sigma^*}(2\sigma^*+1)}\right), \qquad (18)
$$

which is singular in the limit $\sigma_i \to 0$. This shows that these correspond to the non-L^2-integrable part of the expression, and explains why these are ignored.

IV. L^2-BASIS CALCULATIONS

We now try to invert the equation

$$
(H-\sigma I)\tilde{\psi}(x) = x\psi_0(x) \qquad (19)
$$

using a basis of L^2 functions, either a truncated complete set of odd harmonic oscillator states,

$$
\psi^{(n)}(x) = H_{2n-1}(x/b)e^{-x^2/b^2}, \qquad (20)
$$

or a set of odd Gaussian states,

$$
\phi^{(n)}(x) = \frac{(s\alpha^{n-1})^{3/4}}{\sqrt{2}\sqrt[4]{\pi}} x \exp\left(-\frac{1}{2}s\alpha^{n-1}x^2\right), \qquad (21)
$$

we make a finite-dimensional approximation to H and I.

For the orthonormal basis (20) we get

$$
\tilde{\psi}(x) = \sum_{n=1}^{N} c_n(\sigma)\psi^{(n)}(x), \quad d_n = \langle \psi^{(n}|x|\psi_0\rangle \qquad (22)
$$

which gives the equation $(H_{nm}-\sigma\delta_{nm})c_m(\sigma) = d_n$. If we denote the eigenvectors of H in this basis as $\boldsymbol{e}_n$ with eigenvalues λ_n, we see that

$$
L = \left\langle \tilde{\psi}\middle|\tilde{\psi}\right\rangle = \sum_{n=1}^{N} \frac{(\boldsymbol{e}_n\cdot\boldsymbol{d})^2}{(\lambda_n-\sigma_R)^2+\sigma_I^2}, \qquad (23)
$$

and for the Gaussian basis

$$
\tilde{\psi}(x) = \sum_{n=1}^{N} c_n(\sigma)\phi^{(n)}(x), \quad d_n = \langle \phi^{(n)}|x|\psi_0\rangle \qquad (24)
$$

we define a Hamiltonian and overlap matrix by integration from the left with the same basis,

$$
\begin{pmatrix} O_{nm} \\ H_{nm} \end{pmatrix} = \left\langle \phi^{(n}\middle| \begin{pmatrix} 1 \\ H \end{pmatrix} \middle|\phi^{(m)}\right\rangle . \qquad (25)
$$

This gives the equation $(H_{nm}-\sigma O_{nm})c_m(\sigma) = d_n$. If we denote the generalised right-eigenvectors of H in this basis as $\boldsymbol{e}_k$ with eigenvalues λ_k, $H_{nm}(\boldsymbol{e}_k)_m = \lambda_k O_{nm}(\boldsymbol{e}_k)_m$, nornalised as $(\boldsymbol{e}_l)_n O_{nm}(\boldsymbol{e}_k)_m = \delta_{lk}$, we see that again

$$
L = \left\langle \tilde{\psi}\middle|\tilde{\psi}\right\rangle = \sum_{n=1}^{N} \frac{(\boldsymbol{e}_n\cdot\boldsymbol{d})^2}{(\lambda_n-\sigma_R)^2+\sigma_I^2}. \qquad (26)
$$

In the limit $\sigma_I \to 0$ this a a sum of delta functions located at $\sigma_R = \lambda_n$. What we shall do next is analyse the integral of this sum as a function of the "energy" $\omega = \sigma_R$, as a smoother function which we can then approximate by an even smoother one.

There is an obvious saturation issue: The total strength is always equation to

$$
\sum_n (\boldsymbol{e}_n\cdot\boldsymbol{d})^2 \le ||d||^2, \qquad (27)
$$

which is also correct for the non-orthogonal basis.

We now analyse the results for the two basis sets. We have done numerical calculations for harmonic oscillator bases with $b = 1/2, 1, 2, 4$ and 8, see Fig. 2. Since for the numerical calculations the strength T makes a finite jump ($\boldsymbol{d}\cdot\boldsymbol{e}_n$ at the eigenvalue λ_n, there are multiple ways to represent this. What we have chosen is the midway point between these two values, which seems to be overall a very true representation of the analytical result. As we can see from Fig. 2, we can closely mirror the analytic results, apart from for the densest spectrum, $b = 8$, where we see some deviations. This may well be due to the difficulty in doing these calculation, with numerical integration involving up to 2 160th order Hermite polynomials. We clearly see the density of the spectrum increasing, and as we can see in c), the width goes down as b goes up.

Of slightly more interest in the light of the basis we shall use in many of our calculations, is the study of Gaussian states in Fig. 3. We see that in all cased the midpoints of the jumps track the analytical results extremely closely. If we bracket the solutions with the upper and lower values of the jump, we see a width that is roughly constant. That is clearly an enormous overestimate of the error in the results, which are of very high quality. We see that we can achieve as much with 20 Gaussian basis states as with 200 orthornomal ones.

[[Need to analyse the LIT transformation here for finite σ_I]]

Clearly we can also solve the Pöschl-Teller problem for any $\lambda > 1$. Without showing the calculations, we find that for $1 < \lambda < 2$ the convergence is determined by the quality of the description of the first excited state, that now occurs in the same channel as the scattering signal. Even though the total strength is well described, numerically we find a large variation in the strength and position of the bound state when it is very extended (when λ is close to 1).

V. CONCLUSIONS

[1] M. Marchisio, N. Barnea, W. Leidemann, and G. Orlandini, Efficient method for lorentz integral transforms of reaction cross sections, Few-Body Systems **33**, 259 (2003).

[2] V. D. Efros, W. Leidemann, G. Orlandini, and N. Barnea, The lorentz integral transform (LIT) method and its applications to perturbation-induced reactions, Journal of Physics G: Nuclear and Particle Physics **34**, R459 (2007).

[3] G. Pöschl and E. Teller, Bemerkungen zur quantenmechanik des anharmonischen oszillators, Zeitschrift für Physik **83**, 143 (1933).

[4] S. Flügge, *Practical Quantum Mechanics*, Classics in Mathematics (Springer Berlin Heidelberg, 2012).

[5] J. Lekner, Reflectionless eigenstates of the sech^2 potential, American Journal of Physics **75**, 1151 (2007).

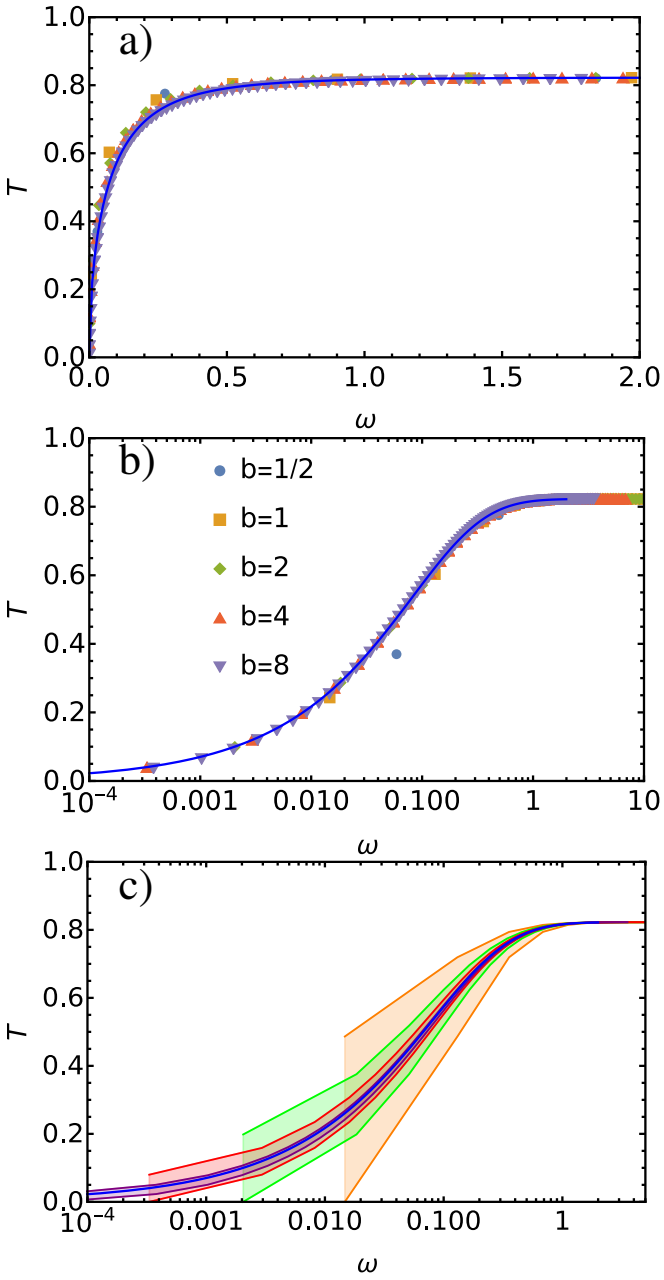

FIG. 2. The cumulative strength for various values of the the harmonic oscillator length parameter. In a) and b) the points plotted are the midpoints of each jump (see main text for details), the only difference between these two figures is the scale. The number of basis functions used is $b = 1/2$: 60, $b = 1$: 50, $b = 2$: 80, $b = 4$: 120 and $b = 8$: 240 In each case the solid blue curve is the analytical result. In c) the lower and upper lines connect the values just before and just after the jumps, respectively. Colours correspond to a) and b) (we do not show $b = 1/2$). Note that the $b = 8$ results seem to lie almost below the exact results. We suspect that this is due to small residual numerical errors in the integration with highly oscillatory states.

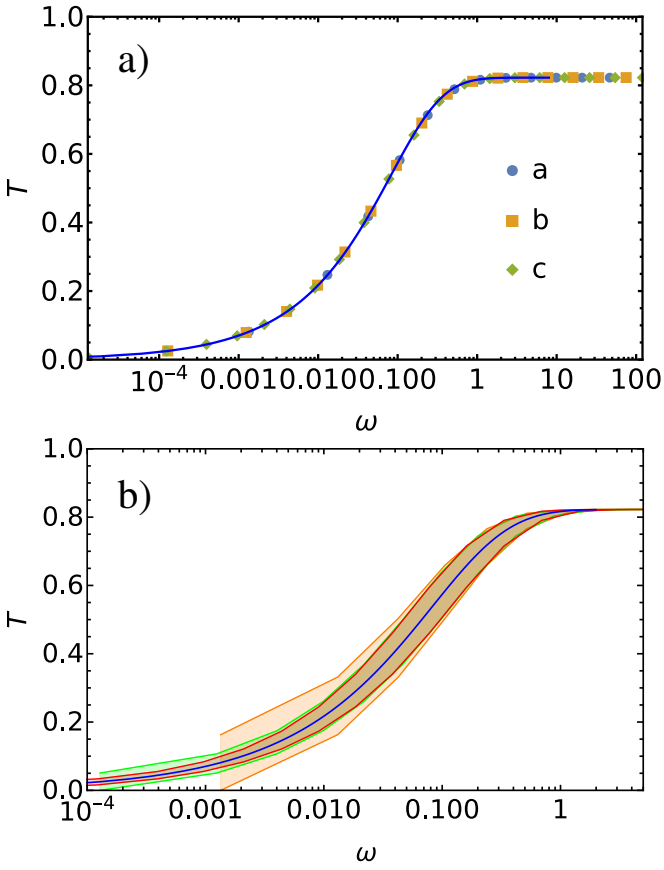

FIG. 3. The convergence of the cumulative strength for a small Gaussian basis (21) for $\alpha = 2$ and a $s = 0.01$ (12 basis functions), b $s = 0.001$ (16 basis functions) and c $s = 0.0001$ (20 basis functions). As in Fig. 2, the points plotted are the midpoints of the jumps.